

Technical University of Denmark



## Nonlocal description of X waves in quadratic nonlinear materials

Larsen, Peter Ulrik Vingaard; Sørensen, Mads Peter; Bang, Ole; Krolikowski, W. Z.; Trillo, S.

*Published in:*

Physical Review E (Statistical, Nonlinear, and Soft Matter Physics)

*Link to article, DOI:*

[10.1103/PhysRevE.73.036614](https://doi.org/10.1103/PhysRevE.73.036614)

*Publication date:*

2006

*Document Version*

Publisher's PDF, also known as Version of record

[Link back to DTU Orbit](#)

*Citation (APA):*

Larsen, P. U. V., Sørensen, M. P., Bang, O., Krolikowski, W. Z., & Trillo, S. (2006). Nonlocal description of X waves in quadratic nonlinear materials. *Physical Review E (Statistical, Nonlinear, and Soft Matter Physics)*, 73(3), 036614. DOI: 10.1103/PhysRevE.73.036614

## DTU Library

Technical Information Center of Denmark

---

### General rights

Copyright and moral rights for the publications made accessible in the public portal are retained by the authors and/or other copyright owners and it is a condition of accessing publications that users recognise and abide by the legal requirements associated with these rights.

- Users may download and print one copy of any publication from the public portal for the purpose of private study or research.
- You may not further distribute the material or use it for any profit-making activity or commercial gain
- You may freely distribute the URL identifying the publication in the public portal

If you believe that this document breaches copyright please contact us providing details, and we will remove access to the work immediately and investigate your claim.

## Nonlocal description of X waves in quadratic nonlinear materials

P. V. Larsen\* and M. P. Sørensen

*Department of Mathematics, Technical University of Denmark, DK-2800 Kongens Lyngby, Denmark*

O. Bang

*COM•DTU, Department of Communications, Optics & Materials, Technical University of Denmark, DK-2800 Kongens Lyngby, Denmark*

W. Z. Królikowski

*Laser Physics Centre and ARC Centre of Excellence for Ultrahigh-Bandwidth Devices for Optical Systems, Research School of Physical Sciences, Australian National University, Canberra, Australian Capital Territory 0200, Australia*

S. Trillo

*Department of Engineering, University of Ferrara, Via Saragat 1, 44100 Ferrara, Italy  
and Istituto Nazionale de Fisica della Materia (INFN)-RM3, Via delle Vasca Navale, 00146 Roma, Italy*

(Received 23 December 2005; published 22 March 2006)

We study localized light bullets and X waves in quadratic media and show how the notion of nonlocality can provide an alternative simple physical picture of both types of multidimensional nonlinear waves. For X waves we show that a local cascading limit in terms of a nonlinear Schrödinger equation does not exist—one needs to use the nonlocal description, because the nonlocal response function does not converge toward a  $\delta$  function. Also, we use the nonlocal theory to show that the coupling to the second harmonic is able to generate an X shape in the fundamental field despite having anomalous dispersion, in contrast to the predictions of the cascading limit.

DOI: [10.1103/PhysRevE.73.036614](https://doi.org/10.1103/PhysRevE.73.036614)

PACS number(s): 03.50.De, 05.45.Yv, 42.65.Jx, 42.65.Tg

### I. INTRODUCTION

Due to their strong and fast nonlinearity, quadratic nonlinear materials have been a center of attention for a number of years. Of particular interest has been the study of localized wave packets, *solitons*, which can act as ideal carriers of optical information. Both spatial [1] (localized in space) and temporal [2] (localized in time) solitons were observed experimentally in quadratic nonlinear materials about a decade ago. More recently, spatiotemporal solitons [3,4], the so-called *light bullets* [5], were also observed.

The existence of light bullets requires materials with anomalous dispersion which, acting similarly to standard diffraction in bulk materials, can counteract nonlinearities of the self-focusing type. Conversely, normally dispersive media support other effects, such as temporal splitting and spectral breaking [4,6,7], that were commonly believed to prevent the existence of nonlinear localized wave packets. However, the perspective changes completely, if one consider so-called *X waves* [8], introduced in the field of linear acoustics. These waves have translationally invariant solutions of the (scalar) linear wave equation with characteristic biconical shape (they are called X because the main longitudinal cut resembles the letter X) [9]. Therefore they exist also as electromagnetic waves whose evidence has been reported both at microwave frequencies [10], and in the context of linear optics [11,12] where they can be considered

nonmonochromatic generalizations of Durnin *et al.*'s Bessel beam [13]. In general, X waves can exist also in vacuum, and do not necessarily have a narrow spectrum. However, when the propagation of beams with narrow spatiotemporal spectral content in bulk dielectrics is considered, linear X waves turn out to be natural eigenmodes of normally dispersive dielectrics [14,15]. Their excitation, however, remains quite difficult because their shape is quite far from standard laser beams. It was therefore a breakthrough when the formation of nonlinear X waves was found starting from a standard Gaussian beam in quadratic nonlinear optical materials [9,16]. The key is that a sufficiently strong nonlinearity provides, through spatiotemporal modulational instability, a mechanism which is able to dynamically evolve a localized input profile into an X wave. General results prove that X waves can have indeed a key role in the nonlinear dynamics both in optics [17–20], and in Bose-Einstein condensation [21,22] where the negative effective mass due to a one-dimensional (1D) lattice mimics the effect of normal dispersion [23].

In quadratic nonlinear, or  $\chi^{(2)}$ , materials, the formation of solitons is not due to a change in refractive index caused by the local intensity of the beam, but due to a cascading phase-modulation mechanism [24]. An intuitive explanation given in Ref. [25] explains some of the occurring phenomena, like soliton formation, self-focusing, and self-defocusing, but it does not explain effects such as soliton interaction and the existence of bound states.

In contrast, the notion of *nonlocality* was recently shown to provide a simple physical explanation of all these effects, as well as of bound states and general soliton interaction

---

\*Electronic address: P.V.Larsen@mat.dtu.dk

[26]. The idea is to describe the effect of the second harmonic (SH) field on the fundamental through a *response function*, which contains the nonlinearity of the system and the linear properties of the SH. This analogy further allows one to obtain analytical solutions of solitons and their bound states in the so-called strongly nonlocal limit, where the governing equations become linear [26–28]. See also Refs. [29,30] for a review of the effects of nonlocality.

Considering only one transverse spatial dimension, it was found in Ref. [26] that with a positive phase mismatch, the response function is localized and symmetric. However, a negative phase mismatch introduces a difference in sign in the SH dispersion relation, which in turn changes the nature of the response function to be oscillatory. This corresponds well with the absence of a continuous family of soliton solutions in this case, where only pairs of solitons exist at discrete points, corresponding to isolated values of the separation between the solitons [31].

Including the temporal dimension in the nonlocal description introduces another way of having opposite signs in the SH dispersion relation, namely, when considering normally dispersive materials. We would thus expect an analogy between systems that support X waves and a nonlocal system with an oscillatory response function.

In this paper we propose a description of (1+2)D X waves [41] in quadratic media, based on a nonlocal response function. The inclusion of the temporal dependence complicates the effect somewhat and the response function turns out to be of Bessel type. Interestingly, we show that for normal SH dispersion the local cascading limit in terms of a nonlinear Schrödinger equation does not exist—one needs to use the nonlocal description, because the nonlocal response function does not converge toward a  $\delta$  function when the degree of nonlocality goes to zero.

Also, we investigate the effects of having opposite signs of the dispersion in the fundamental wave (FW) and SH fields. We demonstrate that X-type waves can form in quadratic nonlinear materials with anomalous dispersion at either the FW or the SH.

## II. GENERAL NONLOCAL SOLITONS

We consider the following standard normalized (all quantities are suitably scaled so that they are dimensionless) model that describes second-harmonic generation under the hypothesis that group-velocity difference is negligible with respect to second-order group-velocity dispersion [32,33]:

$$i\partial_z E_1 + 2\partial_x^2 E_1 + 2d_1 \partial_t^2 E_1 + E_1^* E_2 e^{-i\beta z} = 0, \quad (1)$$

$$i\partial_z E_2 + \partial_x^2 E_2 + d_2 \partial_t^2 E_2 + E_1^2 e^{i\beta z} = 0, \quad (2)$$

where  $E_1$  and  $E_2$  denote the slowly varying amplitude of the fundamental wave and the second harmonic, respectively, and  $\beta$  is the phase mismatch. Important in our context is the sign of  $\beta$  and the dispersion coefficients  $d_1$  and  $d_2$ . Positive values of  $d_{1,2}$  describe anomalous dispersion, the regime for which temporal localization has been reported [3–5], whereas a negative value describes normal dispersion; a re-

quirement for the existence of X waves in the linear case [17].

To obtain simple intuitive predictions it is customary to write the SH as  $E_2 = e_2(x, z, t) \exp(i\beta z)$ , which transforms the SH equation to

$$\beta e_2 - i\partial_z e_2 - \partial_x^2 e_2 - d_2 \partial_t^2 e_2 = E_1^2.$$

For large phase mismatch,  $|\beta| \rightarrow \infty$ , we obtain the *cascading* limit  $e_2 \approx E_1^2/\beta$  (corresponding to neglecting all derivatives of  $e_2$ ), and the (2+1)D nonlinear Schrödinger (NLS) equation for the FW

$$i\partial_z E_1 + 2\partial_x^2 E_1 + 2d_1 \partial_t^2 E_1 + \beta^{-1}|E_1|^2 E_1 = 0, \quad (3)$$

with a local Kerr nonlinearity. It is known that X-wave solutions to the NLS Eq. (3) exist in both the linear and nonlinear cases, provided that  $d_1 < 0$  [17]. The cascading limit corresponds to the situation when the second harmonic is basically slaved to the fundamental wave. However, Eq. (3) with  $e_2 \approx E_1^2/\beta$ , does not accurately describe all the dynamics of the original Eqs. (1) and (2). For example, the (2+1)D NLS equation predicts collapse and modulational instability (MI) for positive  $\beta$  and  $d_1$ , but it is well known that collapse does not exist in  $\chi^{(2)}$  materials [34,35], and that the existence of MI depends on the sign of  $d_2$  [24]. It was recently shown that a nonlocal picture correctly describes these and other effects, such as existence of bound states of solitons, while still providing a simple physically intuitive model for wave interaction [26].

In the nonlocal approach, the only assumption is that  $|\partial_z e_2| \ll |\beta e_2|$ , i.e., that the SH is varying slowly in  $z$ , but without restrictions on the  $x$  or  $t$  dependence. Thus, the nonlocal equations become

$$i\partial_z E_1 + 2\partial_x^2 E_1 + 2d_1 \partial_t^2 E_1 + E_1^* e_2 = 0, \quad (4)$$

$$-\beta e_2 + \partial_x^2 e_2 + d_2 \partial_t^2 e_2 + E_1^2 = 0. \quad (5)$$

Physical insight into the system can be extracted from the spectral domain, and we therefore apply Fourier transformation in both the spatial and temporal domains [ $\tilde{e}_2(k, \omega) = \int \int e_2(x, t) e^{ikx} e^{i\omega t} dx dt$ , where an integration without explicit limits here and henceforth denotes integration from  $-\infty$  to  $\infty$ ], whereby Eq. (5) solves to give

$$\tilde{e}_2 = \frac{1}{\beta} \frac{1}{1 + s_\beta \sigma^2 (k^2 + d_2 \omega^2)} \tilde{E}_1^2 = \frac{1}{\beta} \tilde{R} \tilde{E}_1^2, \quad (6)$$

where  $\tilde{R}$  represents the Fourier-transformed nonlocal response function.  $s_\beta$  is the sign of the phase mismatch, and  $\sigma$  represents the *degree of nonlocality*

$$\sigma = \frac{1}{\sqrt{|\beta|}}. \quad (7)$$

In the simplest case,  $s_\beta = d_2 = +1$ , we see how the cascading limit corresponds to the local limit,  $\sigma \rightarrow 0$ , and that the Fourier-transformed *response function* approaches a constant,  $\tilde{R} = 1$ , which yields the NLS equation (3) discussed above. As we shall see, the case  $s_\beta = -d_2 = 1$  does not have the same simple local (nor nonlocal) limit. This case corresponds

to  $s_\beta=d_2=-1$  with the  $x$  and  $t$  axes interchanged, whereas the case  $s_\beta=-d_2=-1$  is not investigated in this paper.

Furthermore, looking at Eq. (6) we identify the strength of the nonlinearity as

$$\gamma = \frac{1}{\beta} = s_\beta \sigma^2. \quad (8)$$

Interestingly, both the degree of nonlocality and the strength of nonlinearity are determined by  $\sigma$ . Therefore it is not possible to choose these parameters independently.

Substitution of Eq. (6) into Eq. (4) yields the nonlocal equation for the fundamental wave,

$$i\partial_z E_1 + 2\partial_x^2 E_1 + 2d_1\partial_t^2 E_1 + \beta^{-1}N(E_1^2)E_1^* = 0, \quad (9)$$

with the nonlocal nonlinearity determined by

$$N(E_1^2) = \iint R(x-\xi, t-\eta) E_1^2(\xi, \eta, z) d\xi d\eta. \quad (10)$$

Here we see how the nonlinear term is computed by a convolution integral over the product of the squared FW amplitude and the response function  $R$ . The response function in real space is found through a 2D inverse Fourier transform

$$R(x, t) = \frac{1}{4\pi^2} \iint \frac{e^{-ikx} e^{-i\omega t}}{1 + s_\beta \sigma^2 (k^2 + d_2 \omega^2)} dk d\omega. \quad (11)$$

Note how the linear SH properties are incorporated in the response function.

In the strongly nonlocal limit,  $\sigma \gg 1$ ,  $R$  is assumed to be much broader than  $E_1^2$  in Eq. (10) and can therefore be approximated by its Taylor expansion. This makes Eqs. (9) and (10) effectively linear in the form

$$i\partial_z E_1 + 2\partial_x^2 E_1 + 2d_1\partial_t^2 E_1 + \beta^{-1}R(x, t)E_1^* P_1 = 0. \quad (12)$$

Similarly, in the local limit,  $\sigma \ll 1$ ,  $E_1^2$  is assumed to be much broader than  $R$  in order to obtain the NLS equation.

For bright solitary waves  $P_1 = \iint E_1^2(x, t, z) dx dt$ ; for dark solitons  $P_1 = \iint [A_1^2 - E_1^2(x, t, z)] dx dt$ , where  $A_1$  is the background amplitude. The one-dimensional equivalent of Eq. (12) is easily derived, as the response function in this case is readily approximated with its Taylor expansion. In (1+1)D this approximation provides excellent agreement with the full model, except for a narrow region around the origin, where the response function is nondifferentiable [26].

In our (2+1)D case, however, the response function is more complicated. As we shall see, for  $d_2=+1$  a singularity arises at  $(x, t)=(0, 0)$ , whereas for  $d_2=-1$  the response function is singular along hyperbolas in the  $x$ - $t$  plane. When singularities arise, the linearization made for the approximation (12) is no longer valid. This has profound effects for the description of the nonlocal system, e.g., neither accessible solitons [36] nor the cascading limit exists (this is discussed in Sec. V A).

Henceforth, we shall only consider the case of positive phase mismatch,  $s_\beta=+1$ , corresponding to a self-focusing nonlinearity at FW in the cascading limit. The case with negative phase mismatch,  $s_\beta=-1$ , and normal SH dispersion,  $d_2=-1$  is completely analogous to the case  $s_\beta=+1$  and  $d_2$

$=-1$ , but with  $x$  and  $t$  interchanged. The case  $s_\beta=-1$  and  $d_2=+1$ , which gives a circularly shaped singularity in the response function, is not considered here.

### III. LINEAR AND NONLINEAR LENGTH SCALES

As mentioned previously, using a Gaussian input beam profile, X waves have been shown to spontaneously generate in quadratic nonlinear materials [9,37]. Here, we also consider a Gaussian initial condition for the FW

$$E_1(x, t, z=0) = A e^{-(x^2+t^2)/B^2}, \quad (13)$$

where  $B$  determines the spatial and temporal width of the pulse. Let us further consider an unseeded SH, i.e.,  $E_2(x, t, z=0)=0$ . The linear dispersion length of the FW is defined from Eq. (1) without the nonlinear term, as the propagation length at which the width of the amplitude  $|E_1|$  has doubled. This is calculated to be

$$L_D = \frac{\sqrt{3}B^2}{8}. \quad (14)$$

Because there is no seeding of the SH, its linear dispersion length is not relevant.

The nonlinear length associated with wave propagation in the full  $\chi^{(2)}$  system (1) and (2) is more difficult to assess, because it involves nonlinear interaction between two waves according to the equations

$$\partial_z E_1 = iE_1^* E_2 e^{-i\beta z}, \quad \partial_z E_2 = iE_1^2 e^{i\beta z}. \quad (15)$$

In this model there is both an intensity and a phase modulation and which one is dominant depends on  $\beta$  and thus the degree of nonlocality,  $\sigma$ . In general, the nonlinear length  $L_{NL}$  will be the minimum of the nonlinear length obtained from the phase variation  $L_{NL}^{\text{phase}}$  and that obtained from the intensity variation  $L_{NL}^{\text{int}}$ . The exact solution for the SH intensity is

$$|E_2|^2 = u_- \text{sn}^2(\sqrt{u_+} z; k), \quad k = \sqrt{u_-/u_+}, \quad (16)$$

where  $\text{sn}(z; k)$  is the Jacobi elliptic sn function and  $u_\pm$  are given by

$$u_\pm = \frac{1}{8} (8A^2 + \beta^2 \pm \sqrt{16A^2\beta^2 + \beta^4}). \quad (17)$$

The total intensity is conserved, so  $|E_1|^2 = A^2 - |E_2|^2$ . The change in the FW phase  $\phi_1$  is given by

$$\frac{d\phi_1}{dz} = \frac{\beta}{2} \left| \frac{E_2}{E_1} \right|^2. \quad (18)$$

The intensity variation is periodic. Close to phase matching, for  $|\beta| < \sqrt{2A^2}$ , corresponding to  $\sigma^2 > 1/\sqrt{2A^2} = \sigma_{NL}^2$ , the SH intensity can increase to more than half the total intensity  $A^2$ . In this regime, we define the nonlinear length

$$L_{NL}^{\text{int}} = \frac{1}{\sqrt{u_+}} \int_0^{A/\sqrt{2u_-}} \frac{1}{\sqrt{(1-u^2)(1-k^2v^2)}} dv \quad (19)$$

as the propagation length at which the maximum SH intensity has increased to  $A^2/2$ . This nonlinear length, defined



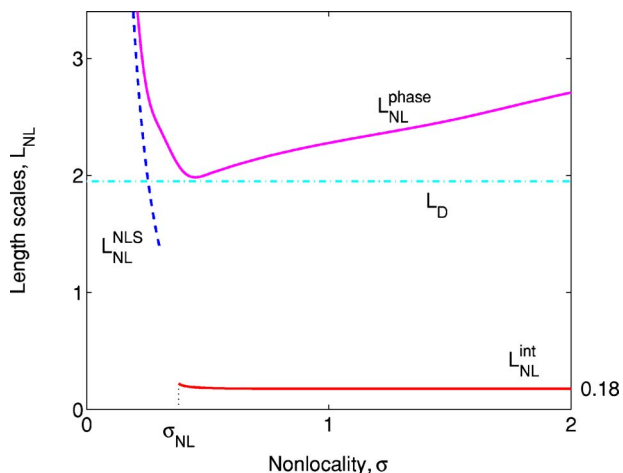


FIG. 1. (Color online) Linear and nonlinear length scales versus the degree of nonlocality,  $\sigma$ , for  $A=5$  and  $B=3$ .

from the intensity variation, tends to the value  $\ln(\sqrt{2}+1)/A$  for  $\sigma \rightarrow \infty$ , i.e., when phase matching is approached. Away from phase matching, for  $|\beta| > \sqrt{2}A^2$ , the SH intensity does not reach half the total intensity and therefore  $L_{NL}^{int}$  is undefined. We note that the threshold of one-half is our choice.

We define the nonlinear length originating from the phase variation,  $L_{NL}^{phase}$ , as the propagation length at which the maximum nonlinear phase shift has reached  $\pi$ . We determine  $L_{NL}^{phase}$  numerically from Eq. (18). A simple analytical expression for  $L_{NL}^{phase}$ , valid for  $\sigma \ll 1$ , can be obtained from the local cascading limit  $i\partial_z E_1 + \beta^{-1}|E_1|^2 E_1 = 0$ . According to this equation, only the phase changes (self-phase modulation); the intensity remains constant. We denote this limiting value of  $L_{NL}^{phase}$  by  $L_{NL}^{NLS}$  and thus  $L_{NL}^{phase} \approx L_{NL}^{NLS} = \pi/\sigma^2 A^2$  for  $\sigma \ll 1$ .

In Fig. 1 we plot the length scales for  $A=5$  and  $B=3$ , which are the values we use in all our simulations. In this case the threshold nonlocality is  $\sigma_{NL}=0.38$  and the linear length is  $L_D \approx 1.95$ .

For  $\sigma > \sigma_{NL}$  the nonlinear length is determined by the intensity variation  $L_{NL} = L_{NL}^{int}$ . For  $\sigma < \sigma_{NL}$  the nonlinear length is determined by the phase  $L_{NL} = L_{NL}^{phase}$ . Thus, in our simulations the nonlinear length is approximately  $L_{NL} = 0.18$  for  $\sigma > 0.38$  and  $L_{NL} = L_{NL}^{phase} > 2.0$  for  $\sigma < 0.38$ . Physically, one does not experience such an abrupt jump; rather it implies that the other measure of  $L_{NL}$  becomes important as well. Interestingly, we find that the nonlinear length related to the phase modulation is always longer than the linear diffraction length. For  $\sigma < 0.2$   $L_{NL}^{NLS}$  is a good approximation of the nonlinear length  $L_{NL}^{phase}$ . At phase matching,  $\beta=0$ , the exact solution to Eq. (15) has no phase variation and correspondingly the nonlinear length  $L_{NL}^{phase}$  must go to infinity for  $\sigma \rightarrow \infty$ , which is confirmed in Fig. 1.

The propagation length should always be viewed relative to these length scales, e.g., stationary states can only be said to be achieved for propagation lengths much longer than both the linear and nonlinear lengths.

#### IV. ACCESSIBLE NONLOCAL (2+1)D SOLITONS; ANOMALOUS SH DISPERSION

In the case of anomalous SH dispersion,  $d_2 > 0$ , the Fourier-transformed response function (6) is positive definite

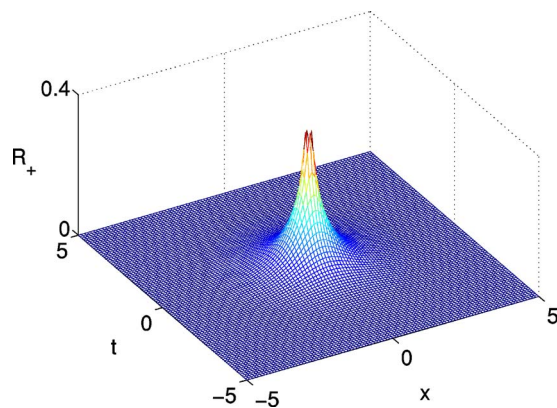


FIG. 2. (Color online) Response function  $R_+(x, t)$  for anomalous SH dispersion, given by Eq. (20). The degree of nonlocality is  $\sigma = 1$ .

(since we consider  $s_\beta = +1$ ) and the response function (11) becomes

$$R_+(x, t) = \frac{1}{2\pi\sigma^2} K_0\left(\frac{1}{\sigma} \sqrt{t^2 + x^2}\right), \quad (20)$$

where  $K_0$  is the modified Bessel function of the second kind of order 0 and the subscript of  $R$  refers to the sign of  $d_2$ . The response function  $R_+$  is depicted in Fig. 2.

In the strongly nonlocal limit, as  $\sigma \rightarrow \infty$ ,  $R_+$  broadens to eventually fill the entire  $x$ - $t$  plane, as illustrated Fig. 3(a). In this limit Eqs. (4) and (5) become effectively linear and are reduced to the form of Eq. (12), because the response function can be approximated by its series expansion. In the (1+1)D case the response function is nondifferentiable at the origin [26], whereas in the (2+1)D spatiotemporal case we

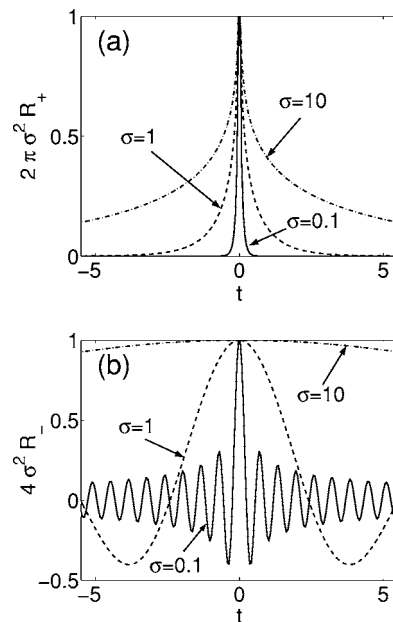


FIG. 3. The effect of nonlocality  $\sigma$  on the response function for both (a) anomalous ( $d_2=1, R_+$ ) and (b) normal ( $d_2=-1, R_-$ ) SH dispersion. Plots are made for constant  $x=0$ .

see that it is undefined at the origin. Nevertheless, the characteristics of the Bessel  $K_0$  function allow us to normalize the response function and thus find a valid expression of the form (12).

Conversely, in the local limit  $\sigma \rightarrow 0$ , corresponding to the cascading limit, the response function approaches a  $\delta$  function, yielding the NLS equation (3) for the FW. We note that for large arguments of  $K_0$  we have the expansion [[38], Eq. (8.451.6)]

$$R_+(x,t) = \frac{1}{\sqrt{8\pi}} \frac{1}{4\sqrt{t^2+x^2}} \frac{1}{\sigma^{3/2}} e^{-\sqrt{t^2+x^2}/\sigma} \left( 1 - \frac{1}{8} \frac{\sigma}{\sqrt{t^2+x^2}} + \dots \right), \quad (21)$$

and we see that for decreasing  $\sigma$ ,  $R_+$  tends to zero for  $(x,t) \neq (0,0)$  and to infinity at  $(x,t)=(0,0)$ . Also, despite the singularity at the origin, the indefinite integral of the modified Bessel function of the second kind,  $K_0$ , is convergent with the value  $2\pi$ . This ensures that the normalization condition

$$\int_{-\infty}^{\infty} \int_{-\infty}^{\infty} R_+(x,t) dx dt = 1 \quad (22)$$

is satisfied, and we have thus shown that  $R_+$  indeed approaches a  $\delta$  function in the local limit. In other words, the conventional cascading limit  $e_2 \approx E_1^2/\beta$  applies also in this (2+1)D case, yielding the (2+1)D NLS Eq. (3).

Originally, the term ‘‘accessible solitons’’ was used to describe the strongly nonlocal linear limit (12) in the case of anomalous SH dispersion [36]. We are using the term *accessible nonlocal solitons* in a broader sense here, where it refers to  $d_2 > 0$  and the whole regime of  $\sigma$  values, because in this case the response function is simple and simple equations and physical explanations may be obtained in both the local and nonlocal limits. As we shall see in Sec. V, this is in contrast to the normal SH dispersion case, where these properties are not present. For normal dispersion we therefore use the term *inaccessible nonlocal solitons*.

Based on the form of the equation for the FW, two separate cases can be considered, namely, the FW dispersion being normal or anomalous, while the SH dispersion is  $d_2 = +1$ . These are discussed in the subsections below.

#### A. Light bullet case: Anomalous FW and anomalous SH dispersion

In the case of anomalous FW dispersion,  $d_1 > 0$ , the well-known light bullets, i.e., waves localized in both time and space, exist [39,40]. The inclusion of the second-harmonic equation will blur the FW somewhat, which might affect the stability of the light bullet, but this aspect is not investigated further here.

#### B. Modified X-wave case: Normal FW and anomalous SH dispersion

We refer to the case of normal FW and anomalous SH dispersion as the *modified X-wave* case because the linear part of the FW equation supports X waves for  $d_1 < 0$  [8,17] and nothing is suggested otherwise based on the cascading

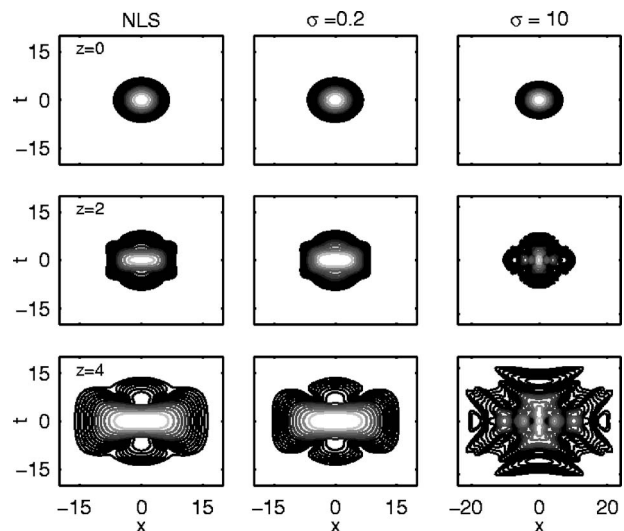


FIG. 4. Intensity profile of the FW,  $|E_1(x,t)|^2$ , at different propagation lengths for the modified X-wave case. Parameter values are  $A=5, B=3, d_1=-1$ , and  $d_2=+1$ . The NLS Eq. (3) solved for  $\sigma=0.2$  (left). Full equations solved for  $\sigma=0.2$  (center) and 10 (right). 15 contour lines from 0.001 logarithmically separated to the maximum intensity.

limit. However, the SH does not support a linear X wave for  $d_2 > 0$  and may affect the X-wave generation. For example, a sufficiently broad response function could make the branches of an X wave in the FW affect each other and thereby either suppress the X wave or alter its cone angle.

To investigate the nonlocal dynamics of X waves we numerically integrated the full dynamical Eqs. (1) and (2) and for comparison also the NLS local cascading limit, given by Eq. (3), with the Gaussian initial condition (13). We have used a Fourier split step method. For Eqs. (1) and (2) the nonlinear part is solved with a fourth-order Runge-Kutta solver. We choose these equations rather than the approximate (4) and (5), or equivalently Eq. (9), for convenience. The validity of the nonlocal approximation is tested in Fig. 10 below. We evolve the equations in  $z$ , with step size  $dz = 0.001$ . This ensures that the energy is constant with a relative deviation of less than  $10^{-10}$ . The simulation box is  $-25 < x, t < 25$ , divided into  $256 \times 256$  grid points unless otherwise stated.

First we consider the dynamics close to the cascading limit where the NLS equation should provide a good approximation. This requires that the width of the response function  $\sigma$  is much smaller than the initial beam width  $B$ . The result of a simulation with  $d_1 = -1$  and  $d_2 = +1$  for  $\sigma = 0.2$  is shown in Fig. 4. In the left column is shown the FW intensity profile of the NLS equation (3) and in the middle column the FW intensity profile of the full model (1) and (2). In this case the dispersion length is  $L_D = 1.95$ , and the nonlinear length  $L_{NL} = L_{NL}^{\text{phase}} \approx 3.7$ . The propagation length  $z=4$  is twice the linear length and only just larger than the nonlinear length. Correspondingly, no stationary state is achieved and no X wave is seen. As expected the two simulations are qualitatively identical.

In Fig. 5 we again compare the full model with the cascading limit NLS equation, but now for  $\sigma=0.5$ , i.e., further

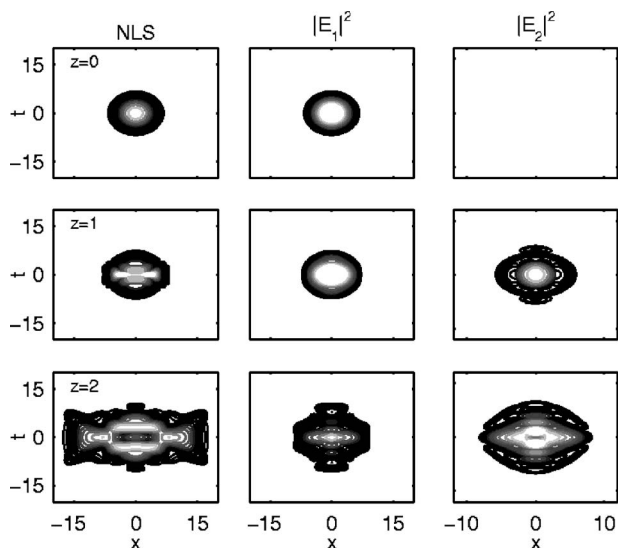


FIG. 5. Intensity profiles at different propagation lengths for the modified X-wave case with nonlocality  $\sigma=0.5$ . Parameter values are  $A=5, B=3, d_1=-1$ , and  $d_2=+1$ . NLS FW Eq. (3) (left). Full equations (1) and (2) solved for  $|E_1(x,t)|^2$  (center) and  $|E_2(x,t)|^2$  (right). 15 contour lines from 0.001 logarithmically separated to the maximum intensity.

away from the cascading limit. Clearly, the cascading limit no longer provides a good approximation. In the NLS model, an X is now more clearly formed than in the case  $\sigma=0.2$  in Fig. 4, because the nonlinear length for  $\sigma=0.5$  is now  $L_{NL}^{NLS}=0.5$ , i.e., much shorter than for  $\sigma=0.2$ , where  $L_{NL}^{NLS}=3.1$ . In contrast, no X evolves from the full model for  $\sigma=0.5$  (middle column of Fig. 5). This is because the nonlinear phase length  $L_{NL}^{phase}=2.0$  and it is just on the border where the nonlinear intensity length sets in.

From Figs. 4 and 5 we see that even in this simple accessible nonlocal soliton case, where the cascading limit exists, the NLS model provides a good approximation only for very small values of  $\sigma \leq 0.2$ . From now on, we consider only the full model (1) and (2) and compare it to the nonlocal model.

From the lengths scales shown in Fig. 1 it is apparent that  $\sigma$  should be larger than 1 to obtain a strong nonlinear and nonlocal attractor, with a small nonlinear length determined by the amplitude,  $L_{NL}=L_{NL}^{int} \approx 0.2$ . Correspondingly, we see no clear X in Fig. 5 for  $\sigma=0.5$  at  $z=2$ . Even though the SH dispersion is anomalous, X waves could be generated in this case as they are supported by the FW [17]. To investigate this we choose good conditions for X-wave generation by using a large degree of nonlocality,  $\sigma=10$ . In Fig. 4 (right column) we now clearly see biconical emission of radiation and it appears as if an X is being formed. In Fig. 6 we continue the propagation out to  $z=8$ , corresponding to four diffraction lengths and 40 nonlinear lengths. In order to avoid problems with radiation reaching the boundaries, this simulation is made on a  $-50 < x, t < 50$  grid with  $360 \times 360$  grid points. An X in the FW is now very clearly observed. In contrast, an X is not formed in the SH and thus a stationary state has not yet been reached.

The degree of nonlocality  $\sigma$  appears in the nonlinear length scale only because it also determines the strength of

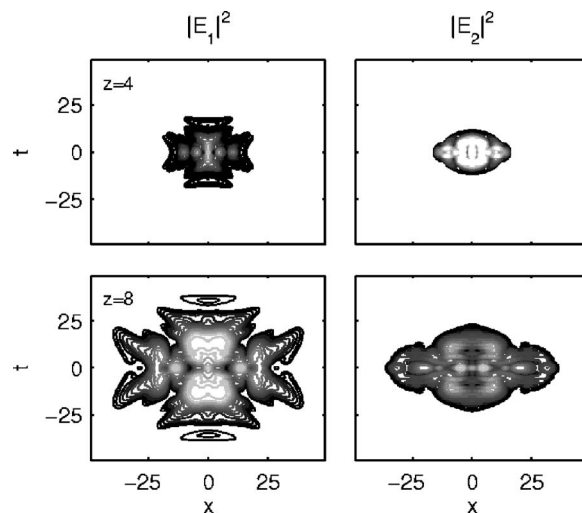


FIG. 6. Intensity profiles for the (left) FW,  $|E_1|^2$ , and (right) SH,  $|E_2|^2$ , at propagation lengths  $z=$  (top) 4 and (bottom) 8. Parameter values are  $A=5, B=3, d_1=-1, d_2=+1$ , and  $\sigma=10$ , i.e., strongly nonlocal. 15 contour lines from 0.005 logarithmically separated to the maximum intensity.

the nonlinearity  $\gamma$ , not because it describes the width of the response function. However, the width of the response function is clearly important, because it determines the (transverse) coupling length over which parts of the beam can feel each other. Because the nonlinearity depends on  $\sigma^2$ , we expect that  $\sigma$  at least should be larger than 1 to generate X waves, because then the nonlinearity is at least of the same order of magnitude as the nonlocality. This is also confirmed in the simulations with  $\sigma=0.2, 0.5$ , and 10, presented in Figs. 4–6.

In any case, the observation of an X wave for  $\sigma=10$  represents evidence of the possibility of X-wave generation in quadratic nonlinear materials with anomalous dispersion at the SH.

### V. INACCESSIBLE NONLOCAL (2+1)D SOLITONS; NORMAL SH DISPERSION

In the case of normal SH dispersion,  $d_2 < 0$ , with positive  $\beta$ , the situation is fundamentally different from the anomalous dispersion case discussed in the previous section. The Fourier-transformed response function is now ( $s_\beta = -d_2 = +1$ )

$$\tilde{R}_-(k, \omega) = \frac{1}{1 + \sigma^2(k^2 - \omega^2)}. \quad (23)$$

Clearly,  $\tilde{R}_-$  now has an X shape, as illustrated in Fig. 7.

The response function in real space,  $R_-$ , becomes [[38], Eqs. (3.723.9) and (3.876.1)]

$$R_-(x, t) = \begin{cases} \frac{1}{4\sigma^2} J_0\left(\frac{1}{\sigma} \sqrt{t^2 - x^2}\right) & \text{for } |x| < |t|, \\ 0 & \text{for } |x| > |t|, \end{cases} \quad (24)$$

where  $J_0$  is the Bessel function of the first kind of zeroth order. We see that the response function in the normally dis-



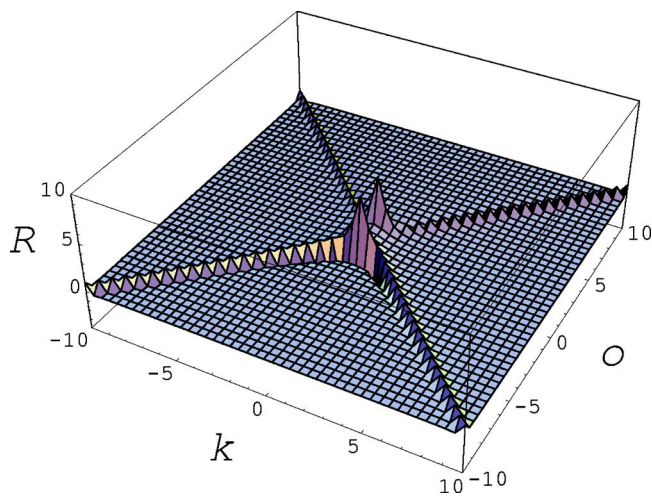


FIG. 7. (Color online) Response function in the Fourier domain,  $\tilde{R}_-(k, \omega)$ , for  $d_2 = -1$ ,  $s_\beta = 1$ , and  $\sigma = 1$ .

persive case is oscillatory in nature and with an X-shaped profile (see Fig. 8). The X shape is given by the lines  $|x| = |t|$  corresponding to where the Fourier-transformed response function  $\tilde{R}_-$  is singular. The cone angle can be determined by linear analysis [14].

The effect of  $\sigma$  for normal SH dispersion is depicted in Fig. 3(b), where  $R_-$  is plotted for constant  $x=0$ . We see how  $\sigma$  governs the oscillation period of the  $J_0$  function and how for sufficiently large values of  $\sigma$ , the central ‘‘hump’’ broadens to engulf the entire domain of definition for the fields. It is thus apparent how  $\sigma$  also describes the degree of nonlocality in the case of  $R_-$  [see Fig. 3(b)].

We note from Eq. (24) that in the real space the response function is undefined along the lines  $|x| = |t|$  (corresponding to  $\omega = \pm \sqrt{1 + \sigma^2 k^2} / \sigma$  in Fourier space). Therefore, the response function is *not* sufficiently smooth and subsequently, the approximation one makes to obtain the strongly nonlocal linear limit is not valid here. Thus no accessible solitons are expected, in contrast to the case of anomalous SH dispersion.

For large arguments,  $R_-$  can be approximated as [[38], Eq. (8.451.1)]

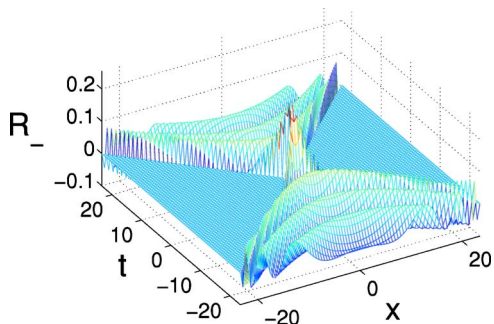


FIG. 8. (Color online) The response function  $R_-(x, t)$  [Eq. (24)] in the normally dispersive case  $d_2 = -1$  for  $\sigma = 1$ . Compare with Fig. 2.

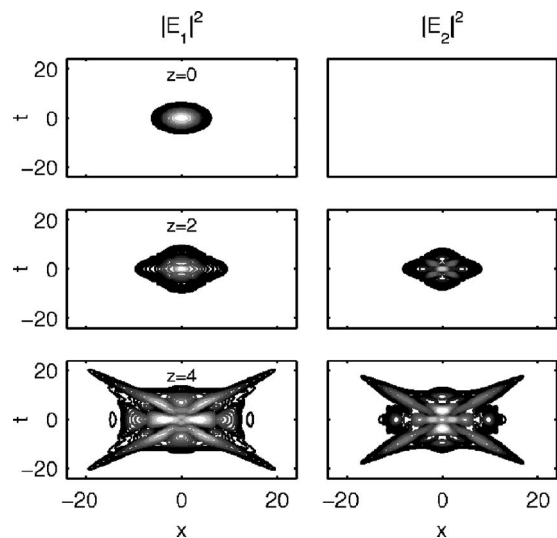


FIG. 9. Intensity profile of the strongly nonlocal X-wave case,  $\sigma = 10$ . The evolution of  $|E_1|^2$  (left) and  $|E_2|^2$  (right). Parameter values are  $A=5, B=3$ , and  $d_1 = d_2 = -1$ . 15 contour lines from 0.005 logarithmically separated to the maximum intensity.

$$R_-(x, t) = \frac{\sigma^{-3/2}}{\sqrt{8\pi}} \frac{1}{\sqrt{t^2 - x^2}} \cos\left(\frac{\sqrt{t^2 - x^2}}{\sigma} - \frac{\pi}{4}\right). \quad (25)$$

For simplicity, consider the case  $x=0$ . We see that as  $\sigma \rightarrow 0$ ,  $R_-$  tends to infinity if  $t$  is small. But we also see that for larger  $t$ , the response function does not approach zero in this limit. Hence we do not recover a  $\delta$  function in the local limit for normal SH dispersion. This means that the cascading limit is not applicable in this case.

More formally, the normalization integral can be calculated as [[38], Eq. (6.517)]

$$\int_{-t_0}^{t_0} \left( \int_{-\infty}^{\infty} R_-(x, t) dx \right) dt = 1 - \cos\left(\frac{t_0}{\sigma}\right), \quad (26)$$

and we see that as  $t_0$  goes to infinity, the value of the normalization integral oscillates between 0 and 2 for fixed  $\sigma$ ; hence X-wave spatiotemporal beams are not normalizable [17].

Thus, normal SH dispersion is fundamentally different from the anomalous case, since the response function does not have a  $\delta$ -function (cascading) limit for  $\sigma \rightarrow 0$ , nor is it smooth enough to formally allow for a strongly nonlocal linear limit,  $\sigma \rightarrow \infty$ , and nor is it normalizable. We therefore use the term *inaccessible nonlocal solitons* for the localized wave solutions with normal SH dispersion.

#### A. X-wave case: Normal FW and SH dispersion

Here the linear equations for the FW and SH both support X waves and we know that X waves can be generated [9,37]. The generation of an X wave is shown in Fig. 9 in the strongly nonlocal regime for  $\sigma = 10$ . The left (right) column depicts the evolution of the FW (SH) intensity at propagation lengths  $z=0, 2$ , and 4. The length scales are  $L_D = 1.95$  and  $L_{NL} = L_{NL}^{\text{int}} \approx 0.2$ .



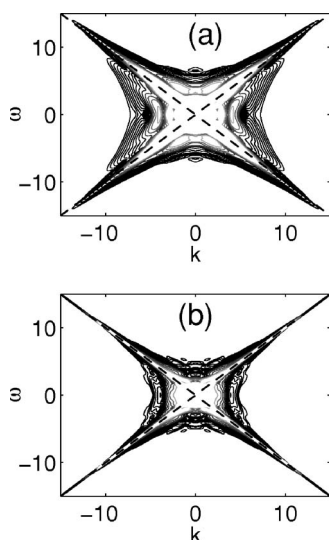


FIG. 10. Comparison between  $|\widetilde{E}_2|^2$  (a) and the nonlocal prediction  $(1/\beta)^2 |\widetilde{E}_1|^2 |\widetilde{R}|^2$  (b) at  $z=4$  with 25 logarithmically spaced contours between 0.0001 and 10. Parameter values are  $A=5, B=3$ , and  $d_1=d_2=-1$ .  $\sigma=10$ , i.e., strongly nonlocal. Dashed lines correspond to  $\sigma\omega = \pm\sqrt{1+\sigma^2 k^2}$ .

We see how the initial Gaussian pulse evolves into a clear X-shaped pattern in both the FW and SH fields. Even though  $z=4$  is only about two diffraction lengths it corresponds to about 20 nonlinear lengths, and with a good degree of certainty we say that a stationary two-color X wave can be obtained in this case. By “two-color” we mean that the X appears in both the FW and SH. Note that also the spectra evolve into X shapes (see Fig. 10).

To investigate the validity of the nonlocal description of X waves, we perform a numerical simulation of the full two-component model (1) and (2) and obtain  $|E_1|^2$  and  $|E_2|^2$ . Our nonlocal theory predicts that we might as well have solved the single-component nonlocal equation (9) for the fundamental and then found the SH according to the relation (6). In other words, the nonlocal model predicts that the FW and SH spectral intensities are linked through the relation  $|\widetilde{E}_2|^2 = |\frac{1}{\beta} \widetilde{R} \widetilde{E}_1|^2$ .

In Fig. 10 we show spectral intensities for the SH,  $|\widetilde{E}_2|^2$ , at  $z=4$  for  $\sigma=10$ , corresponding to the SH at  $z=4$  in Fig. 9, and compare it the nonlocal prediction  $|\frac{1}{\beta} \widetilde{R} \widetilde{E}_1|^2$ . We see that the key features of the X wave are essentially captured, even though the widths differ somewhat. The correspondence might become better after further propagation and evolution towards a stationary state. A cone angle of  $90^\circ$  is expected from both linear and nonlinear theory [17]. We further see that the hyperbola branches of the X obey the nonlocal relation  $\omega^2 = \sigma^{-2} + k^2$  and are thus separated by  $2\sigma^{-2} = 0.02$  at  $k=0$ . From standard linear theory and the cascading limit this separation would be equal to twice an undetermined propagation constant. Our nonlocal model predicts a fixed and predetermined separation of  $2\sigma^{-2}$ , which our simulations confirm. Correspondingly, the nonlocal model is indeed a reasonable approximation in this strongly nonlocal case with  $\sigma=10$ .

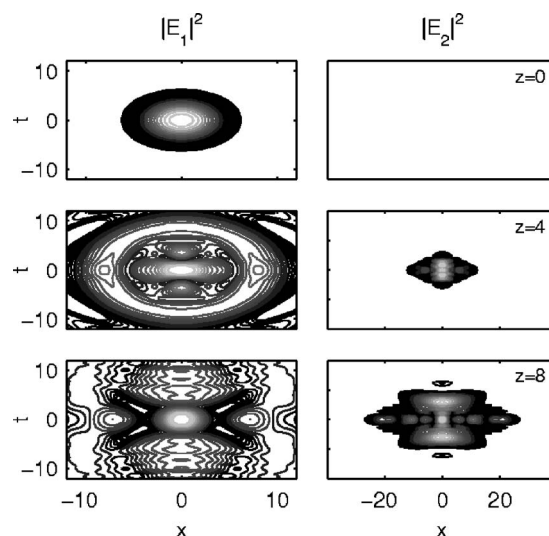


FIG. 11. FW and SH intensity profiles  $|E_1|^2$  (left) and  $|E_2|^2$  (right) at propagation lengths  $z=0, 4$ , and  $8$ . Parameter values are  $A=5, B=3$ , and  $d_1=-d_2=1$ . Strongly nonlocal case,  $\sigma=10$ . 25 contour lines from 0.005 logarithmically separated to the maximum intensity. The mesh size is 360 on a  $-50 < x, t < 50$  domain.

We note that due to the singularities of the response function it is hard to obtain a more precise measure for the validity of the nonlocal model.

### B. Modified light bullet case: Anomalous FW and normal SH dispersion

In analogy with Sec. IV B, we denote this case the modified light bullet case, because the linear part of the FW equation supports light bullet generation, not X waves, and nothing is suggested otherwise based on the cascading limit. In contrast, the X-shaped response function of the nonlocal model for  $d_2=-1$  indicates the whole new possibility of generation of a two-color X wave, despite the anomalous FW dispersion. We stress that this X wave in the FW is not predicted by linear theory or the cascading limit. Furthermore, this X-wave generation would occur despite the FW being initially Gaussian and the SH being unseeded, thus only through the nonlocal nonlinear attractor, which prevails over the FW linear properties.

We consider again the strongly nonlocal case with  $\sigma=10$ . In Fig. 11 we show the results of a simulation of the full model out to  $z=8$ , corresponding to about four diffraction lengths and 40 nonlinear lengths. We have used a larger computational box ( $-50 < x, t < 50$ ) in order to be able to simulate for longer distances, because the generation of an X wave requires the built up of the unseeded SH and is thus expected to be slow. We use  $360 \times 360$  discretization points to maintain a reasonable resolution. From the figure we see a lot of radiation in the FW during the buildup of the SH which at  $z=8$  has grown sufficiently strong to indeed generate an X in the FW despite its dispersion being anomalous.

## VI. CONCLUSION

We have developed a nonlocal description of (2+1)-dimensional spatiotemporal waves in quadratic non-

linear materials. The model predicts that the interaction between the FW and SH is described by a response function which takes into account the linear properties of the SH. The nonlocal model is therefore more accurate than the cascading limit NLS equation, which neglects all linear properties of the SH and assumes that the SH is simply slaved to the FW.

Depending on the linear properties of the SH, the response function can take on three fundamentally different shapes, characterized by having singularities either at the origin, along hyperbolas, or along circles in the spectral domain. In this work we have limited ourselves to a positive phase mismatch, which excludes the type of response function with a circular singularity.

With a positive phase mismatch and anomalous SH dispersion the response function of the nonlocal model has nice physical properties: it is normalizable and it has both a simple local (cascading) and strongly nonlocal linear limit. We therefore denote the localized wave solutions of this case as accessible nonlocal solitons (including X waves).

In contrast, for normal SH dispersion, we have shown that the response function is not normalizable and that it neither has a cascading limit nor a strongly nonlocal linear limit. We therefore term the localized wave solutions of this case as inaccessible nonlocal solitons (including X waves). Our nonlocal model predicts the general tendency of X waves to form in this case, even for anomalous FW dispersion; an effect that is never predicted by the cascading limit, which only predicts light bullets.

We have calculated the linear and nonlinear length scales and shown how they vary with the degree of nonlocality. We have shown the existence of two nonlinear lengths defined

from the nonlinear phase and intensity variations, respectively. For a small degree of nonlocality the phase change determines the nonlinear length and for strong nonlocality the intensity variation determines the nonlinear length. The threshold between the two regimes has been found.

We have conducted numerical simulations with an unseeded SH and a Gaussian FW input. The simulations show that the nonlocal model provides a reasonable description of the dynamics in a broad range of parameter values.

We have shown that accessible nonlocal X waves can be generated for normal FW dispersion and anomalous SH dispersion. For normal SH dispersion we have shown that inaccessible nonlocal X waves can be generated both for normal FW dispersion (conventional X waves) and for anomalous FW dispersion.

We have shown the generation of two-color X waves in quadratic nonlinear materials with anomalous dispersion in either the FW or SH. The inaccessible nonlocal X wave found here with anomalous FW dispersion is predicted neither by linear theory nor by the cascading limit. However, both these types of X waves arise naturally in the framework of the nonlocal model.

#### ACKNOWLEDGMENTS

The authors wish to thank Dr. D. Edmundson, ANU Supercomputer Facility, Australian National University, Canberra ACT 0200, Australia, for computational advice. We acknowledge financial support from the Danish Natural Science Research Council through Project No. 21-02-0500 (MIDIT).

- 
- [1] W. E. Torruellas, Z. Wang, D. J. Hagan, E. W. VanStryland, G. I. Stegeman, L. Torner, and C. R. Menyuk, *Phys. Rev. Lett.* **74**, 5036 (1995).
  - [2] P. Di Trapani, D. Caironi, G. Valiulis, A. Dubietis, Danielius, and A. Piskarskas, *Phys. Rev. Lett.* **81**, 570 (1998).
  - [3] X. Liu, L. J. Qian, and F. W. Wise, *Phys. Rev. Lett.* **82**, 4631 (1999).
  - [4] H. S. Eisenberg, R. Morandotti, Y. Silberberg, S. Bar-Ad, D. Ross, and J. S. Aitchison, *Phys. Rev. Lett.* **87**, 043902 (2001).
  - [5] F. Wise and P. D. Trapani, *Opt. Photonics News* **13**, 28 (2002).
  - [6] J. K. Ranka, R. W. Schirmer, and A. L. Gaeta, *Phys. Rev. Lett.* **77**, 3783 (1996).
  - [7] A. A. Zozulya, S. A. Diddams, A. G. Van Engen, and T. S. Clement, *Phys. Rev. Lett.* **82**, 1430 (1999).
  - [8] J. Lu and J. F. Greenleaf, *IEEE Trans. Ultrason. Ferroelectr. Freq. Control* **39**, 441 (1992).
  - [9] C. Conti, S. Trillo, P. Di Trapani, G. Valiulis, A. Piskarskas, O. Jedrkiewicz, and J. Trull, *Phys. Rev. Lett.* **90**, 170406 (2003).
  - [10] D. Mugnai, A. Ranfagni, and R. Ruggeri, *Phys. Rev. Lett.* **84**, 4830 (2000).
  - [11] H. Sönajalg, M. Rätsep, and P. Saari, *Opt. Lett.* **22**, 310 (1997).
  - [12] P. Saari and K. Reivelt, *Phys. Rev. Lett.* **79**, 4135 (1997).
  - [13] J. Durnin, J. J. Miceli, and J. H. Eberly, *Phys. Rev. Lett.* **58**, 1499 (1987).
  - [14] M. A. Porras, S. Trillo, C. Conti, and P. D. Trapani, *Opt. Lett.* **28**, 1090 (2003).
  - [15] M. A. Porras and P. Di Trapani, *Phys. Rev. E* **69**, 066606 (2004).
  - [16] O. Jedrkiewicz, J. Trull, G. Valiulis, A. Piskarskas, C. Conti, S. Trillo, and P. Di Trapani, *Phys. Rev. E* **68**, 026610 (2003).
  - [17] C. Conti, *Phys. Rev. E* **70**, 046613 (2004).
  - [18] M. Kolesik, E. M. Wright, and J. V. Moloney, *Phys. Rev. Lett.* **92**, 253901 (2004).
  - [19] A. Dubietis, E. Gaizauskas, G. Tamosauskas, and P. Di Trapani, *Phys. Rev. Lett.* **92**, 253903 (2004).
  - [20] S. Droulias, K. Hizanidis, J. Meier, and D. N. Christodoulides, *Opt. Express* **13**, 1827 (2005).
  - [21] L. Khaykovich, F. Schreck, G. Ferrari, T. Bourdel, J. Cubizolles, L. D. Carr, Y. Castin, and C. Salomon, *Science* **296**, 1290 (2002).
  - [22] K. E. Strecker, G. B. Partridge, A. G. Truscott, and R. G. Hulet, *Nature (London)* **417**, 150 (2002).
  - [23] C. Conti and S. Trillo, *Phys. Rev. Lett.* **92**, 120404 (2004).
  - [24] A. V. Buryak, P. D. Trapani, D. V. Skryabin, and S. Trillo, *Phys. Rep.* **370**, 63 (2002).
  - [25] G. Assanto and G. Stegeman, *Opt. Express* **10**, 388 (2002).
  - [26] N. I. Nikolov, D. Neshev, O. Bang, and W. Z. Królikowski,

- Phys. Rev. E **68**, 036614(R) (2003).
- [27] I. V. Shadrivov and A. A. Zharov, *J. Opt. Soc. Am. B* **19**, 596 (2002).
- [28] C. Conti, M. Peccianti, and G. Assanto, *Phys. Rev. Lett.* **91**, 073901 (2003).
- [29] W. Krolikowski, O. Bang, N. I. Nikolov, D. Neshev, J. Wyller, J. J. Rasmussen, and D. Edmundson, *J. Opt. B: Quantum Semiclassical Opt.* **6**, S288 (2004).
- [30] W. Krolikowski, O. Bang, J. Wyller, and J. J. Rasmussen, *Acta Phys. Pol. A* **103**, 133 (2003).
- [31] A. V. Buryak and Y. S. Kivshar, *Phys. Lett. A* **197**, 407 (1995).
- [32] C. R. Menyuk, R. Schiek, and L. Torner, *J. Opt. Soc. Am. B* **11**, 2434 (1994).
- [33] O. Bang, *J. Opt. Soc. Am. B* **14**, 51 (1997).
- [34] L. Bergé, V. K. Mezentsev, J. J. Rasmussen, and J. Wyller, *Phys. Rev. A* **52**, R28 (1995).
- [35] L. Bergé, O. Bang, J. J. Rasmussen, and V. K. Mezentsev, *Phys. Rev. E* **55**, 3555 (1997).
- [36] A. W. Snyder and D. J. Mitchell, *Science* **276**, 1538 (1997).
- [37] P. Di Trapani, G. Valiulis, A. Piskarskas, O. Jedrkiewicz, J. Trull, C. Conti, and S. Trillo, *Phys. Rev. Lett.* **91**, 093904 (2003).
- [38] I. Gradshteyn and I. Ryzhik, *Table of Integrals, Series, and Products* (Academic, New York, 1980).
- [39] D. E. Edmundson and R. H. Enns, *Opt. Lett.* **17**, 586 (1992).
- [40] D. E. Edmundson and R. H. Enns, *Phys. Rev. A* **51**, 2491 (1995).
- [41] Here (1+2)D means that diffraction is effective in only one transverse dimension, say  $x$ , as occurs in planar waveguides. Linear X waves have been investigated in this case by D. N. Christodoulides, N. K. Efremidis, P. Di Trapani, and B. A. Malomed, *Opt. Lett.* **29**, 1446 (2004); A. Ciattoni and P. Di Porto, *Phys. Rev. E* **69**, 056611 (2004).